TCAD MODELING OF TLM CONTACT RESISTANCE STRUCTURES

Geoffrey Gregory[1], Siyu Guo[1], Andrew M. Gabor[2], Adam M. Payne[3], Kristopher O. Davis[1], Rob Janoch[2], Andrew Anselmo[2]

[1]Florida Solar Energy Center – University of Central Florida
[2]BrightSpot Automation LLC
[3]Suniva Inc.
[1]1679 Clearlake Road, Cocoa, FL, USA 32922-5703, Tel: +1-321-638-1000, Fax: +1-321-638-1010
Email: ggregory@fsec.ucf.edu
[2]5 Abbot Mill Lane 10F, Westford, MA, USA 01886, Tel: +1-508-633-5413
[3]5765 Peachtree Industrial Boulevard, Norcross, GA, USA 30092, Tel: +1-404-477-2700

ABSTRACT: The TLM approach to measuring contact resistivity is commonly performed to help optimize cell designs, materials, and processing recipes, and for use in quality control at the factory. Despite the popularity of the technique, there are no standards on how to perform the measurement or how to prepare the structures. In order to better understand the method and its sensitivities to the physical characteristics of its test structures, we have constructed TCAD and circuit simulator models for the measurement sample. The models correctly predict trends in the measured contact resistivity as the sample width is varied. The models also show how the TLM is affected by the presence of unprobed contacts when measuring solar cells. The results are used to create correction factors that can be incorporated into the TLM measurement.
Keywords: contact resistance, TLM, photovoltaic cells

1 INTRODUCTION

As metallization processes improve in the crystalline silicon solar cell industry, it is important that the study of contact resistivity is well developed. The traditional technique for measuring contact resistivity is the TLM approach, which was first introduced by Berger [1]. To prepare test structures, either a special structure is fabricated with variable spacing between the contacts, or a standard solar cell is cut into strips parallel to the busbars. Resistance values are then measured between pairs of contacts on the strips. When using strips cut from cells, contacts can be skipped over to achieve the variable spacing.

We previously [2] explored the dependence of these measurements on sample preparation methods and found a dependence of the measured contact resistivity on the sample width. When sample widths are high ($\sim 25\ mm$) there is a tendency for the measured contact resistivity to be overestimated. When samples are large and/or the contacts are narrow, the voltage drop down the length of the contact can be significant such that error is introduced to the measurement. Similarly, when sample widths are low ($\sim 5\ mm$) there is a tendency for the measured contact resistivity to be overestimated. This effect may be due to the mechanism of edge shunting, which is most likely to occur when the ratio of strip perimeter length to strip area is high.

Additionally, the idea of skipping over contacts to achieve variable spacings was not fully captured within the original TLM theory, and it is possible that significant error could result from current entering unprobed contacts as the current flows across the strip. Finally, the firing process for forming silver paste contacts on solar cells might damage the emitter underneath the contacts, thus increasing the sheet resistance there, or selective emitter structures could be implemented that lower the sheet resistance in the contact regions. These factors are also not captured by the original TLM theory.

There is a need to quantify the trends that contact resistivity measurements exhibit as sample preparation methods vary, and to modify the calculations in order to take into account the effects mentioned above. In the present study, we first describe the fundamentals of the TLM method and provide an overview of a useful semi-automatic tool, the *ContactSpot*, used to perform this measurement. We present a numerical, physically based three dimensional model along with a circuit analysis detailing the effects of strip width on contact resistivity measurements. We compare these two models to experimental data acquired using the *ContactSpot* and make conclusions regarding optimal sample conditions for the TLM method. The models are also used to create to create correction factors that can be incorporated into the TLM measurement.

2 TLM TECHNIQUE

Consider the fitted curve shown below in Fig. 1. When performing the TLM technique, the total resistance R_T between two contacts of length W and width f is measured and plotted as a function of contact spacing d. Three parameters can be extracted from this plot: the contact resistance R_C, the sheet resistance ρ_{sh}, and the transfer length L_T. The value of the total resistance at the y-intercept of the plot is $2\ R_C$. Given this value, the effective contact resistivity $\rho_{c\text{-}eff}$ can be calculated using the area of the contact segments ($W * f$). As contact spacing d increases, the effect of the sheet resistance on the total resistance measurement increases, thus creating the slope of the TLM plot. Therefore, the value of sheet resistance can be extracted using:

$$R_T / d = \rho_{sh} / W \tag{2.1}$$

The value of the contact spacing at the intercept where $R_T = 0$ yields $2\ L_T$. The transfer length found here indicates how much of the contact width is actually being used to insert current into the semiconductor. This can be used in place of the contact width f to calculate an actual contact resistivity.
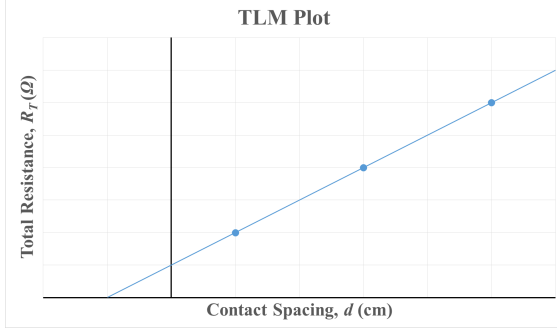
Figure 1: Fitted curve of total resistance versus contact spacing.

Table I: Definitions

Parameter	Definition	Units
ρ_c	Contact resistivity	$m\Omega\text{-}cm^2$
$\rho_{c\text{-}eff}$	Effective contact resistivity	$m\Omega\text{-}cm^2$
ρ_{sh}	Sheet resistance	$\Omega/\square$
R_c	Contact resistance	Ω
W	Sample width	mm
F	Contact width	mm
L_T	Transfer length	mm
R_T	Total resistance	Ω
D	Contact spacing	cm

The *ContactSpot* is a semi-automatic tool for performing contact resistivity measurements. Fig. 2 shows a photo of two *ContactSpot* units. This unit includes a sample platform and microscope with translation and rotation controls for easy contact alignment. Each probe head contains 10 sets of current and voltage probes allowing the measurement of 10 contacts at a time.

This tool can also be used to measure the line resistance of contact segments. During this measurement current is probed along the length of a contact and the resultant voltage is then measured. The resistance of the metal can then be calculated and used to find a value of resistance per unit length.

Figure 2: Two *ContactSpot* tools for measuring contact resistivity

As an example of distortions seen measuring strips from solar cells, Fig. 3 shows the results of an experiment where we measured $\rho_{c\text{-}eff}$ versus strip width on the *ContactSpot* for several Suniva solar cells. High values of $\rho_{c\text{-}eff}$ were seen when the strip widths went above 15 *mm* and below 10 *mm*. When strip widths are low (~ 5 *mm*) the ratio of the sample's perimeter length to area is high. In this case, effects such as edge shunting and recombination may cause the measured $\rho_{c\text{-}eff}$ to be artificially high. Issues with the conductivity of contacts may also skew the measured values, especially when the

TLM structure's strip width is high (~ 25 *mm*). We explore these and other effects below by modeling the system.
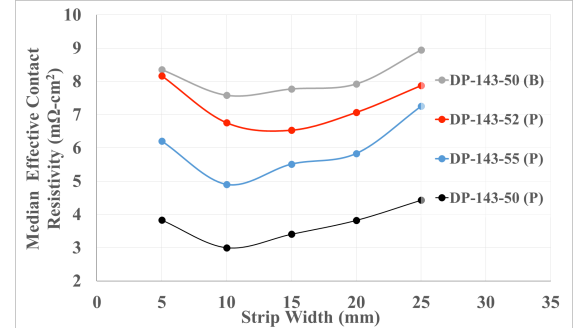
Figure 3: Plot of $\rho_{c\text{-}eff}$ versus strip width measured on strips cut from Suniva cells.

3 PHYSICAL MODEL AND CIRCUIT SIMULATOR

We used the physically based device simulator, Silvaco Atlas®, to model of the TLM test samples. This TCAD software allows the user to define the physical structure to be simulated, the physical models to be used, and the bias conditions for which the electrical characteristics are to be simulated [4]. Table 2 shows a list of the parameters we used to create the TLM structure model. These parameters are typical values measured on silicon solar cells.

**Table II:** TCAD and Circuit Model Base Parameters

Parameter	Value	Units
Contact resistivity, ρ_c	2	$m\Omega\text{-}cm^2$
Sheet resistance, ρ_{sh}	85.0	$\Omega/\square$
Sample width, W	5.0 - 25.0	mm
Contact width, f	60.0	μm
Contact spacing, d	0.175	cm
Current level, I	0.01	A
Emitter thickness, t	0.3	μm

Silvaco Atlas® requires that each structure be defined on a mesh that covers the physical simulation domain. In order for the model to yield an accurate solution, it is important that the mesh is defined properly. Therefore, a very fine mesh is defined near the metal-semiconductor interface and then made coarse away from the contacts for the sake of computational efficiency.

We created the circuit simulation using LTspice IV software. The parameters used for simulation are the same as those used in the TCAD model, shown in Table 2. The two models are compared quantitativley in order to verify the accuracy of the solutions.

It's possible that edge shunting effects may be introducing significant amounts of error in the TLM results. When current is injected into a contact, it can find a path of low resistance through the structure along the edge of the sample. In order to determine whether edge shunting introduces error into the TLM measurement, we incorporated the mechanism into the models. Fig. 4 shows a plot of $\rho_{c\text{-}eff}$ versus strip width for structures containing shunt paths. We also implemented structures without the shunt in order to quantify the impact of this phenomenon on the measured $\rho_{c\text{-}eff}$. Both models show that the edge shunt modifies the measured value of $\rho_{c\text{-}eff}$

at all strip widths. The most notable effect is at a low strip width of 5 mm.
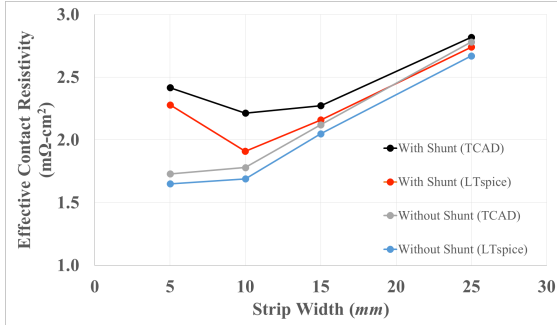
Figure 4: Plot of $\rho_{c\text{-eff}}$ versus strip width for TLM structures with and without shunt paths.

It can be seen that for both the structure with an edge shunt and the one without an edge shunt, the $\rho_{c\text{-eff}}$ increases with increasing strip width. In order to investigate the cause of this phenomenon, we created three structures using the base parameters given in Table 2. We then defined different line resistance values for each structure's metal contacts. This was done to study the effect that the line resistance of the contacts has on the measured $\rho_{c\text{-eff}}$. Fig. 5 shows the value of $\rho_{c\text{-eff}}$ measured for each combination of input parameters.
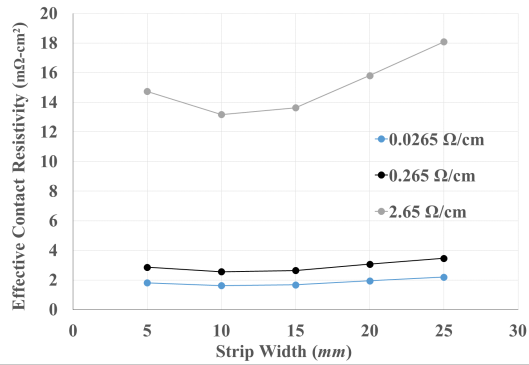
Figure 5: TCAD simulation of $\rho_{c\text{-eff}}$ versus strip width for varying line resistance values of the contacts.

It can be seen that the trends in increasing $\rho_{c\text{-eff}}$ are most pronounced for the structures with high line resistance (2.65 Ω/cm), and the measured value approaches the input contact resistivity (2 $m\Omega\text{-}cm^2$) as the line resistance of the contacts decreases.

When standard solar cells are used for contact resistivity measurements it is necessary to skip over contacts in order to measure the total resistance R_T at different contact spacings d. In the past, groups [3] have reported seeing consistently higher values of ρ_c when using TLM structures with large amounts of unprobed contacts (> 5). There is a concern for the effect of the unprobed contacts that are skipped over during the resistance measurements of the TLM. In order to study this effect, we modeled TLM structures using the base parameters from Table 2, and each structure was then used to measure $\rho_{c\text{-eff}}$ with and without the unprobed contacts. We also modeled structures with varying amounts of contacts in order to see how the quantity of unprobed contacts would affect the measurement. The results of this simulation can be seen below in Fig. 6.
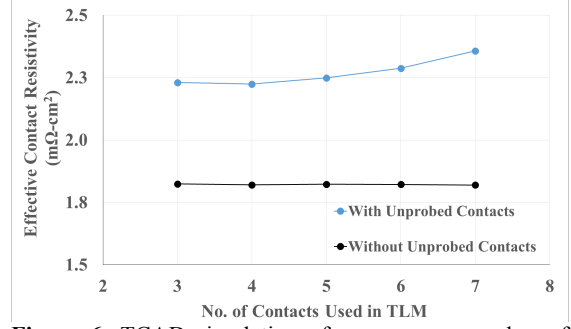

Figure 6: TCAD simulation of $\rho_{c\text{-eff}}$ versus number of contacts on the TLM structure.

Fig. 6 shows that $\rho_{c\text{-eff}}$ remains relatively stable for the structures that did not have unprobed contacts. For the structures that did have unprobed contacts, the $\rho_{c\text{-eff}}$ does increase as the number of contacts used to create the TLM plot increases. The simulated $\rho_{c\text{-eff}}$ is always higher for the structures containing unprobed contacts than the structures that did not contain them.

4 RESULTS AND DISCUSSION

The plot in Fig. 4 shows a high value of $\rho_{c\text{-eff}}$ at the lowest strip width (5 mm) for the structure that has a shunt path incorporated into the models. This plot indicates that edge shunting does skew the measured $\rho_{c\text{-eff}}$ most notably when the ratio of strip perimeter length to strip area is high. The measured value is skewed since the shunt paths decrease the value of R_T at each point in the TLM plot. This will decrease the slope of the plot and increase the value at the y-intercept, $2R_c$.

The same plot also shows that the simulated value of $\rho_{c\text{-eff}}$ increases as the width of the sample increases. This increase is a result of an additional voltage drop along the probed contacts that the TLM does not account for. We used the circuit simulator to show the voltage drop along a probed contact (Fig. 7). As the contacts become longer, the voltage drop gets larger, and a higher measured $\rho_{c\text{-eff}}$ is obtained. This is verified in Fig. 5, where the effect is amplified as the line resistance of the contacts increases. If the contact is unable to effectively conduct the injected current, then voltage will have a significant drop along the length of the contact, making the current flow more concentrated towards its center.
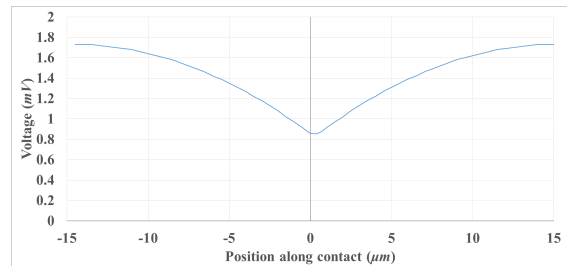
Figure 7: Plot of voltage along the length of a contact from circuit simulation.

As trends in metallization steadily move toward narrower, less conductive contacts, it is necessary to correct for the line resistance of the metal in order to obtain more accurate $\rho_{c\text{-eff}}$ measurements. From simulation results, we observed that current flow through the contacts always has a linear decrease/increase (shown in Fig. 8).
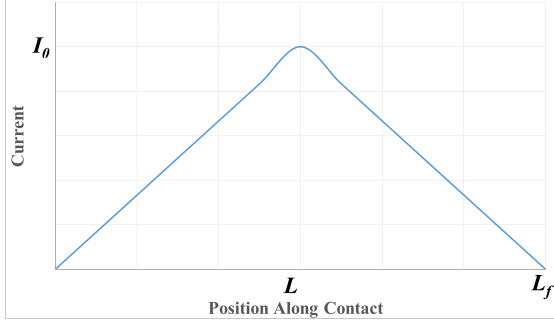
Figure 8: Plot of current flow versus position within a contact.

Assuming the total injection current is I_0, the current flow to each direction is $I_0/2$. The voltage drop from the edge of a contact to its center can be calculated by integration:

$$V_{drop} = \int_0^L \left(\frac{I_0}{2} \times \frac{x}{L}\right) \rho_l \, dx = \frac{\rho_l L I_0}{4} \tag{4.1}$$

where ρ_L is the metal line resistance in Ω/cm, I_0 is injection current in A, and L is half of the full contact length L_f in cm. Assuming the voltage drop to be equal along both halves of the contact, we calculate the total voltage drop to be:

$$V_{total} = \int_0^L \left(\frac{I_0}{2} \times \frac{x}{L}\right) \rho_l \, dx = \frac{\rho_l L I_0}{4} \times 2 = \frac{\rho_l I_0 L_l}{4} \tag{4.2}$$

From this, the additional resistance caused by the current flow through the contact can be calculated:

$$R = \frac{V_{total}}{I_0} = \frac{\rho L_f}{4} \tag{4.3}$$

This value can then be subtracted from the measured contact resistance R_c in order to obtain a more accurate value of $\rho_{c\text{-eff}}$.

Another factor which influences the measured $\rho_{c\text{-eff}}$ is the current flow through the unprobed contact, which is not accounted for in the original TLM technique. As is shown in Fig. 6, the existence of unprobed contacts in a total resistance measurement will increase the final value of $\rho_{c\text{-eff}}$. As each unprobed contact is added to a TLM structure, the current path becomes more conductive. If the sheet resistance ρ_{sh} of the sample is low, then current will have a propensity to enter into the intermediate contacts as it travels through the sample. We used the circuit model to determine the percentage of current that flows through the unprobed contacts as a function of sheet resistance for a given value of $\rho_{c\text{-eff}}$ (Fig. 9).
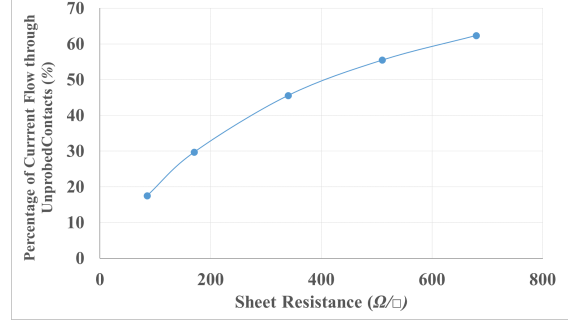
Figure 9: Circuit simulation of percentage of current flow through the unprobed contacts as a function of sheet resistance.

By knowing the percentage of current that flows through the unprobed contacts, we can determine the true voltge drop between two contacts. Assuming 20% of the total injected current flows through the unprobed contacts, the true voltage drop will be 80% of the measured voltage drop. We then adjust the contact width f to $0.8f$, which corrects the value of $\rho_{c\text{-eff}}$ to a more accurate result. Fig. 10 shows a plot of $\rho_{c\text{-eff}}$ at different strip widths before and after correction.
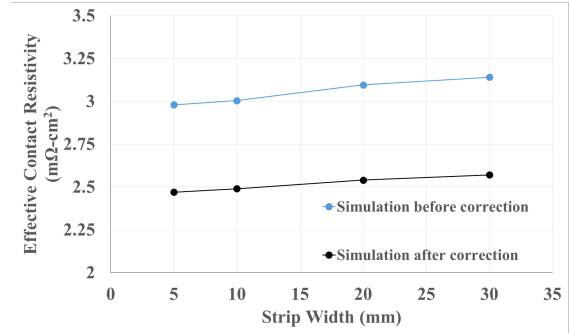
Figure 10: Circuit simulation of $\rho_{c\text{-eff}}$ versus strip width before and after being corrected for the existence of unprobed contacts

5 CONCLUSIONS

We have performed the first TCAD and circuit simulations that we are aware of for TLM contact resistivity structures, and thus we have observed errors due to edge shunting effects, voltage drop along the contacts, and the existence of unprobed contacts. Both the correction for the voltage drop along the contact and the correction for current entering unprobed contacts can be incorporated into tools like the *ContactSpot*. These corrections will increase the viability of the TLM technique as contacts become narrower and less conductive and as emitter or BSF sheet resistance increases.

We have shown with our models that edge shunting introduces a considerable error in the measured $\rho_{c\text{-eff}}$ at low strip widths. For our structures, the strip width should be kept higher than 5mm in order to avoid this effect, but in general this will likely depend on the cell structure and the strip preparation method.

REFERENCES

[1]   Berger, H. H. (1972). "Models for contacts to planar devices." Solid-State Electronics 15: 145-158.
[2]   A.M. Gabor, G. Gregory, A. Payne, R. Janoch, A. Anselmo, V. Yelundur, and K. O Davis, *Dependence of Solar Cell Contact Resistivity Measurements on Sample Preparation Methods,* in 43rd *IEEE Photovoltaics Specialist Conference.* 2016, IEEE: Portland, OR, USA. (Not yet published)
[3]   R. Janoch, A.M. Gabor, A. Anselmo, and C.E. Dube, et al., *Contact Resistance Measurement-Observations on Technique and Test Parameters,* in 42nd *IEEE Photovo,ltaic Specialist Conference.* 2015, IEEE: New Orleans, LA, USA.
[4]   Silvaco International (2015), "Atlas User's Manual, Device Simulation Software." Pg. 25.